CHINESE OPTICS LETTERS

Vol. 19, No. 11 | November 2021

Wideband chaos generation based on a dual-mode microsquare laser with optical feedback

Chunguang Ma (马春光)[1,2], Jiliang Wu (吴冀亮)[1,2], Jinlong Xiao (肖金龙)[1,2], Yongtao Huang (黄勇涛)[1,2], Yali Li (李亚理)[1,2], Yuede Yang (杨跃德)[1,2*], and Yongzhen Huang (黄永箴)[1,2]

[1] State Key Laboratory of Integrated Optoelectronics, Institute of Semiconductors, Chinese Academy of Sciences, Beijing 100083, China

[2] Center of Materials Science and Optoelectronics Engineering, University of Chinese Academy of Sciences, Beijing 100049, China

*Corresponding author: yyd@semi.ac.cn

Received February 18, 2021 | Accepted April 7, 2021 | Posted Online August 16, 2021

We propose and demonstrate the generation of wideband chaos based on a dual-mode microsquare semiconductor laser with optical feedback. By adjusting the dual-mode intensity ratio and the feedback strength, wideband chaos covering more than 50 GHz in the RF spectrum is achieved. The standard and effective bandwidths of the chaotic signal are 31.3 GHz and 30.7 GHz with the flatness of 8.3 dB and 6.1 dB, respectively.

Keywords: dual-mode laser; micro laser; chaos; optical feedback.

DOI: 10.3788/COL202119.111401

1. Introduction

Chaotic lasers have attracted a lot of attention and received intensive investigation for their applications in random bit generation[1–3], chaos-based communication[4,5], optical time domain reflector[6,7], and chaotic lidar[8,9]. The chaotic bandwidth is one significant parameter, as high bandwidth can improve the performance of the chaotic laser in terms of the generation rate of the chaotic signal[9–11]. However, owing to the limitation of the relaxation-oscillation frequency of semiconductor lasers, the chaotic bandwidth of the chaotic semiconductor laser with optical feedback is typically restricted to several gigahertz[12,13].

Several approaches utilizing two or more lasers have been proposed to break through the limitation of relaxation-oscillation frequency and enhance the chaotic bandwidth, e.g., injecting chaotic signals from one laser to another laser[12], using three-cascaded semiconductor lasers[14], or mutually injected semiconductor lasers[15]. To simplify the system and improve the reliability, wideband chaos was generated from a single laser by carefully designing the laser chip or the feedback loop[16,17]. Pan *et al.* demonstrated the wideband chaos generation based on a monolithic three-section laser[16]. Yang *et al.* improved the bandwidth and flatness of the chaotic signal with a single laser by using an active optical feedback loop combined with a high nonlinear fiber[17].

In this Letter, we propose a wideband chaos generation system with a single-cavity dual-mode microsquare laser. The intensity ratio between the dual lasing modes can be tuned by adjusting the biased current of the microsquare laser. Based on the dual-mode microsquare laser with balanced intensity, wideband chaos with a standard bandwidth of 31.3 GHz is realized by tuning the feedback strength. Benefiting from the simple structure of the dual-mode laser, the system is easy to implement without tuning multiple currents.

2. Experimental Setup

Figure 1 shows the experimental setup for wideband chaotic signal generation. The dual-mode microsquare semiconductor laser is mounted on a thermoelectric cooler (TEC) to fix the working temperature. The output light from the laser is collected by a single-mode fiber (SMF) and then coupled into a feedback loop with a length of 51.4 m. The feedback loop contains an optical circulator (OC) to guide the light out and into the laser, an erbium-doped fiber amplifier (EDFA) with maximum output power of 10 dBm, and an optical bandpass filter (OBPF) to amplify and filter out the optical signal at the target wavelength, as shown in Fig. 2(d). The OBPF (BVF-200CL, Alnair Labs) has a tunable bandwidth of 0.1–13 nm and an insertion loss of 3.5 dB. Besides, a polarization controller (PC) is utilized to control the polarization. The optical signal is divided into two equal parts by a 50/50 optical splitter. One part is for the feedback loop, and the other part is converted to an electric signal by a high-speed photodetector (PD) [XPDV21x0(RA)]. The electric RF signal is then measured by a 50 GHz electric spectrum analyzer (ESA) (R&S FSWP50).

3. Results

Figure 2(a) shows the microscopic image of a microsquare semiconductor laser composed of a square microcavity with an

© 2021 Chinese Optics Letters

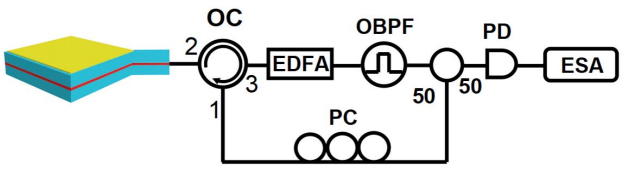

Fig. 1. Experimental setup for wideband chaotic signal generation based on dual-mode microsquare laser. OC, optical circulator; EDFA, erbium-doped fiber amplifier; OBPF, optical bandpass filter; PD, photodetector; PC, polarization controller; ESA, electric spectrum analyzer.

output waveguide[18]. The side length of the square cavity and the width of the waveguide are 18 and 1.5 μm, respectively. The laser is fabricated on an InP-based multi-quantum-well wafer using a similar technique as that in Ref. [19]. The working temperature of the microsquare laser is fixed by setting TEC temperature at 293 K. The microsquare laser has a threshold of 8 mA. The spectral linewidth of the main lasing peak at 31 mA is about 35 MHz, which is a typical value for the dual-mode microsquare laser[20]. The representative lasing spectra at the injection currents of 31, 40, 50, and 51 mA are shown in Fig. 2(b). With the increase of the biased current, a transfer from single-transverse-mode lasing to dual-transverse-mode is observed around 1535 nm. The intensity ratio between the two modes decreases from 39.3 dB to ~0 dB and the current increases from 31 to 51 mA. The lasing mode interval remains about 0.23 nm at 50 and 51 mA, and two small side peaks are four-wave mixing peaks. Figure 2(c) shows the different magnetic field distributions of the fundamental and first-order transverse modes in the microsquare laser corresponding to the two lasing modes in Fig. 2(b). Different longitudinal modes have similar field patterns and a wavelength interval $\Delta\lambda_l = \lambda^2/(2\sqrt{2}an_g)$, where a is the side length of the square, and n_g is the group index[21]. Figure 2(d) shows that the longitudinal modes have a free spectral range of 12.55 nm, which is in accordance with the theoretical prediction.

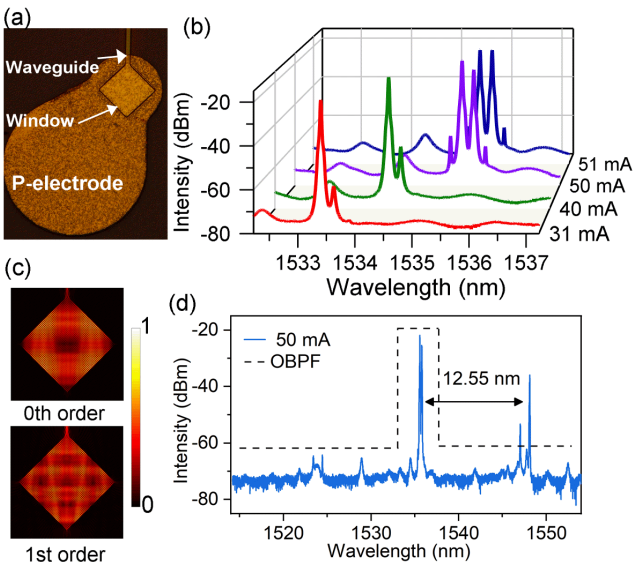

Fig. 2. (a) Microscopic image of the microsquare laser. (b) Representative lasing spectra of the microsquare laser. (c) Magnetic field distributions of the fundamental (zeroth-order) and first-order (1st-order) mode. (d) Lasing spectrum at 50 mA in a large scale to show the longitudinal mode characteristics and the function of the OBPF.

The SMF coupled optical power from the laser is about 70 μW at 50 mA, and an EDFA is used to amplify the feedback optical power. The feedback strength is defined as the ratio of the optical power entering port 1 of the OC to the output power of the laser. The measured RF spectra at different currents are presented in Fig. 3 at the feedback strength of 7.3 dB. At 31 mA, the RF spectrum shows a broad peak at about 8.9 GHz related to the relaxation-oscillation frequency of the microsquare laser. Because the two transverse modes have a large intensity ratio of 39.3 dB, the RF spectra are similar to that measured with a single-mode laser. With the increase of biased current, the intensity of the mode at the longer-wavelength side increases, as shown in Fig. 2(b), and, hence, the peak at the frequency of ~29 GHz related to the mode beating emerges in the RF spectra. The peak intensity increases from −80.68 to −67.5 dB as the biased current increases from 40 to 50 mA. At 51 mA, wideband chaos generation with a relatively flat spectrum is obtained, as the two modes have near equal intensity.

The standard bandwidths of the chaotic signal versus the biased currents are plotted in Fig. 4 as red circles. The standard bandwidth is defined as the range between the DC and the frequency that contains 80% of the RF spectral power[22]. When the current increases from 31 to 51 mA, the standard bandwidth is enhanced from 11.9 to 28.2 GHz, which shows that the dual-transverse-mode state provides an enhancement factor of about 2.5 for the bandwidth compared to the single-transverse-mode state. The standard bandwidth appears to slightly drop at 51 mA compared to that at 50 mA, which is consistent with the drop of the beating-frequency peak in Fig. 3. Correspondingly, due to the spreading of the peak power, the flatness, defined as the difference between the maximum and minimum spectral values within the standard (effective) bandwidth[23], is improved from 12.3 to 10.2 dB, as shown in the inset of Fig. 4. Besides, the blue squares in Fig. 4 show the continuous change of the mode intensity ratio versus the current from 31 to 51 mA.

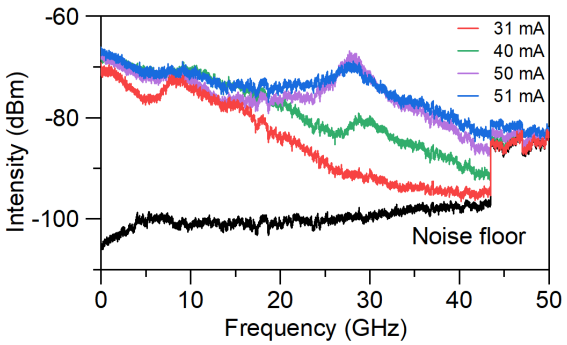

Fig. 3. RF spectra of the generated chaotic signal at different currents with fixed feedback strength of 7.3 dB.

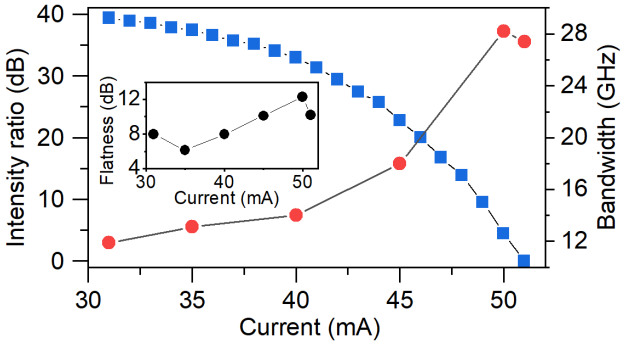

Fig. 4. Intensity ratio between two lasing modes (blue squares) and standard bandwidth (red circles) of the chaotic signal versus the biased currents. Inset: flatness of the RF spectrum versus biased current.

At a biased current of 51 mA, optical spectra are measured under different feedback strengths and plotted in Fig. 5, which are vertically shifted by 5 dB for clarity. When the feedback strength decreases from 7.3 dB to 3.8 dB by adjusting the amplification rate of the EDFA, the −10 dB linewidth of the short (long)-wavelength mode decreases from 0.16 (0.15) to 0.07 (0.06) nm.

The RF spectra with different feedback strengths are shown in Fig. 6(a). As the feedback strength decreases from 7.3 to 0.8 dB, both the mode-beating peak and the relaxation-oscillation peak become narrow[24], the depressions between the two peaks become deep, and the flatness of the spectrum becomes worse from 10.9 dB to 21 dB, as indicated by the red circles in Fig. 6(b). The standard bandwidth remains almost unchanged during the tuning of the feedback strength, as indicated by blue squares in Fig. 6(b), because the standard bandwidth is mainly determined by the strong mode-beating peak due to the definition of the standard bandwidth. In fact, the standard bandwidth cannot describe the bandwidth of the spectrum with multiple peaks accurately. Then, the effective bandwidth is introduced to characterize the chaotic signal, as indicated by blue triangles in Fig. 6(b). The effective bandwidths sum up large discrete spectral segments accounting for 80% of the total power[25].

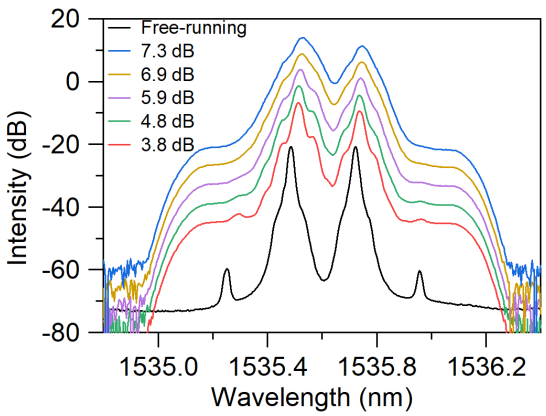

Fig. 5. Lasing spectra of the microsquare laser with a fixed biased current of 51 mA and different feedback strengths.

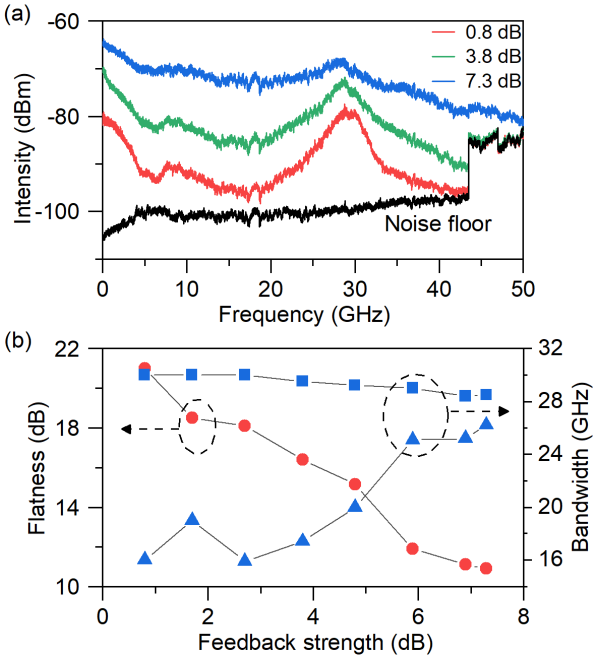

Fig. 6. (a) Representative RF spectra with different feedback strengths at 51 mA. (b) Flatness in the standard bandwidth, standard bandwidth, and effective bandwidth as a function of the feedback strength, indicated by symbols of red circles, blue squares, and blue triangles.

When the feedback is weak, the peaks are narrow, and small ranges of frequencies with large RF power can contain 80% of the total power, leading to the reduction of the effective bandwidth (16 GHz at feedback strength of 0.8 dB). The RF spectrum becomes flat with the increase of feedback, and the effective bandwidth increases to approach the standard bandwidth.

Besides, the RF spectral level decreases with the feedback strength decrease, which is because the detuning of the feedback strength by EDFA also reduces the optical power into the PD.

The above results show that wideband chaos can be generated based on the dual-mode microsquare laser. A flat RF spectrum can be obtained with balanced dual-mode lasing and high feedback strength. To further improve the flatness, we replace the 50/50 optical splitter by an 80/20 one with the 80% power feedback to the laser to increase the feedback strength (10.3 dB). A flatter chaotic signal covering more than 50 GHz in the spectrum is obtained as shown in Fig. 7(a). The spectrum is distinctly higher than the noise floor, which is typical for chaotic signals. The standard bandwidth of the RF spectrum is 31.3 GHz with a flatness of 8.3 dB. The effective bandwidth of the RF spectrum is 30.7 GHz with a flatness of 6.1 dB. Besides, the low frequency components rise because of the competition of the modes[26]. The time series and the corresponding autocorrelation function (ACF) of the chaotic signal are presented in Figs. 7(b) and 7(c), respectively. The time series shows noise-like oscillation in sub-nanoseconds, and the ACF is expressed as a Dirac delta function, which is typical for the chaotic state. Besides, the ACF curve has a correlation peak at 257.5 ns, which is related to the feedback loop time.

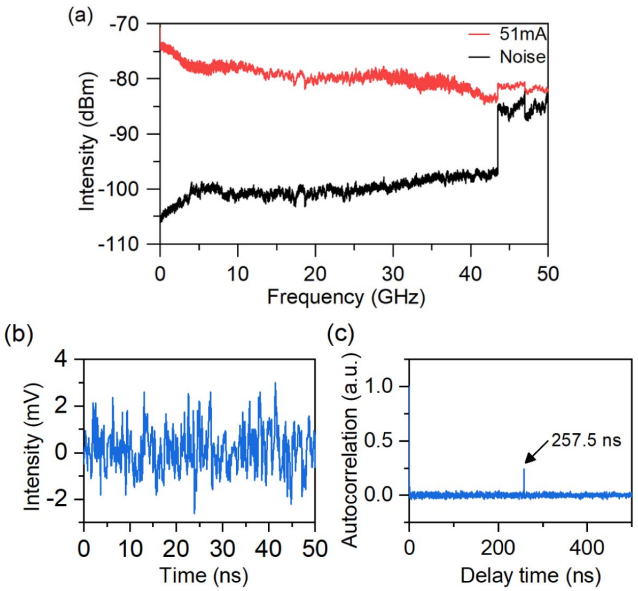

Fig. 7. (a) RF spectrum with feedback strength of 10.3 dB at 51 mA. (b) Time series and (c) autocorrelation coefficient of the chaotic signal.

The microsquare laser is designed for dual-mode lasing with a mode interval of about 30 GHz[19], which is appropriate for wideband chaotic signals[16]. When the modes are far apart from each other, the depression in the middle range should be extremely deep, which cannot be eliminated by increasing the feedback strength due to the limitation of the mode linewidth[24]. To further enhance the bandwidth of the chaotic signal, one possible solution is to design a three-mode laser and construct multiple beating peaks in the spectrum. Thus, the depression can be eliminated.

4. Conclusion

In conclusion, we have proposed and demonstrated the generation of wideband chaotic signals based on a dual-mode microsquare laser under optical feedback. By adjusting the feedback strength to 10.3 dB and the intensity ratio of the two modes to 0 dB, a wideband chaotic signal covering more than 50 GHz in the RF spectrum can be achieved. The standard bandwidth and the effective bandwidth of the chaotic signal are 31.3 GHz and 30.7 GHz with flatness of 8.3 dB and 6.1 dB, respectively. The chaotic signal with wide bandwidth and good flatness, generated from a single-cavity dual-mode laser with optical feedback, demands a good match of the dual-mode intensity ratio and feedback strength. The principle also implies that chaotic signals with higher bandwidth and better flatness can be achieved by utilizing a three or multimode laser with optical feedback, which is important for better applications of chaotic lasers.

Acknowledgement

This work was supported by the National Natural Science Foundation of China (Nos. 61935018 and 61874113).

References

1. M. Sciamanna and K. A. Shore, "Physics and applications of laser diode chaos," Nat. Photon. **9**, 151 (2015).
2. A. Uchida, K. Amano, M. Inoue, K. Hirano, S. Naito, H. Someya, I. Oowada, T. Kurashige, M. Shiki, S. Yoshimori, K. Yoshimura, and P. Davis, "Fast physical random bit generation with chaotic semiconductor lasers," Nat. Photon. **2**, 728 (2008).
3. P. Li, Y. Guo, Y. Guo, Y. Fan, X. Guo, X. Liu, K. Li, K. A. Shore, Y. Wang, and A. Wang, "Ultrafast fully photonic random bit generator," J. Lightwave Technol. **36**, 2531 (2018).
4. M. Li, Y. Chen, Y. Song, C. Zeng, and X. Zhang, "DOE effect on BER performance in MSK space uplink chaotic optical communication," Chin. Opt. Lett. **18**, 070601 (2020).
5. J. Ke, L. Yi, G. Xia, and W. Hu, "Chaotic optical communications over 100-km fiber transmission at 30-Gb/s bit rate," Opt. Lett. **43**, 1323 (2018).
6. X. Wang, S. Li, X. Jiang, J. Hu, M. Xue, S. Xu, and S. Pan, "High-accuracy optical time delay measurement in fiber link," Chin. Opt. Lett. **17**, 060601 (2019).
7. Z. Hu, B. Wang, L. Wang, T. Zhao, H. Han, Y. Wang, and A. Wang, "Improving spatial resolution of chaos OTDR using significant-bit correlation detection," IEEE Photon. Technol. Lett. **31**, 1029 (2019).
8. F. Y. Lin and J. M. Liu, "Chaotic lidar," IEEE J. Sel. Top. Quantum Electron. **10**, 991 (2004).
9. Y. Xiao, T. Deng, Z.-M. Wu, J.-G. Wu, X.-D. Lin, X. Tang, L.-B. Zeng, and G.-Q. Xia, "Chaos synchronization between arbitrary two response VCSELs in a broadband chaos network driven by a bandwidth-enhanced chaotic signal," Opt. Commun. **285**, 1442 (2012).
10. I. Reidler, Y. Aviad, M. Rosenbluh, and I. Kanter, "Ultrahigh-speed random number generation based on a chaotic semiconductor laser," Phys. Rev. Lett. **103**, 024102 (2009).
11. I. Kanter, Y. Aviad, I. Reidler, E. Cohen, and M. Rosenbluh, "An optical ultrafast random bit generator," Nat. Photon. **4**, 58 (2010).
12. K. Hirano, T. Yamazaki, S. Morikatsu, H. Okumura, H. Aida, A. Uchida, S. Yoshimori, K. Yoshimura, T. Harayama, and P. Davis, "Fast random bit generation with bandwidth-enhanced chaos in semiconductor lasers," Opt. Express **18**, 5512 (2010).
13. Y. Wang, Z. Jia, Z. Gao, J. Xiao, L. Wang, Y. Wang, Y. Huang, and A. Wang, "Generation of laser chaos with wide-band flat power spectrum in a circular-side hexagonal resonator microlaser with optical feedback," Opt. Express **28**, 18507 (2020).
14. R. Sakuraba, K. Iwakawa, K. Kanno, and A. Uchida, "Tb/s physical random bit generation with bandwidth-enhanced chaos in three-cascaded semiconductor lasers," Opt. Express **23**, 1470 (2015).
15. L. Qiao, T. Lv, Y. Xu, M. Zhang, J. Zhang, T. Wang, R. Zhou, Q. Wang, and H. Xu, "Generation of flat wideband chaos based on mutual injection of semiconductor lasers," Opt. Lett. **44**, 5394 (2019).
16. B. Pan, D. Lu, and L. Zhao, "Broadband chaos generation using monolithic dual-mode laser with optical feedback," IEEE Photon. Technol. Lett. **27**, 2516 (2015).
17. Q. Yang, L. Qiao, M. Zhang, J. Zhang, T. Wang, S. Gao, M. Chai, and P. M. Mohiuddin, "Generation of a broadband chaotic laser by active optical feedback loop combined with a high nonlinear fiber," Opt. Lett. **45**, 1750 (2020).
18. H. Long, Y.-Z. Huang, X.-W. Ma, Y.-D. Yang, J.-L. Xiao, L.-X. Zou, and B.-W. Liu, "Dual-transverse-mode microsquare lasers with tunable wavelength interval," Opt. Lett. **40**, 3548 (2015).
19. Y.-D. Yang and Y.-Z. Huang, "Mode characteristics and directional emission for square microcavity lasers," J. Phys. D **49**, 253001 (2016).
20. H.-Z. Weng, Y.-Z. Huang, X.-W. Ma, F.-L. Wang, M.-L. Liao, Y.-D. Yang, and J.-L. Xiao, "Spectral linewidth analysis for square microlasers," IEEE Photon. Technol. Lett. **29**, 1931 (2017).
21. H.-Z. Weng, Y.-D. Yang, J.-L. Wu, Y.-Z. Hao, M. Tang, J.-L. Xiao, and Y.-Z. Huang, "Dual-mode microcavity semiconductor lasers," IEEE J. Sel. Top. Quantum Electron. **25**, 1501408 (2019).
22. H. Someya, I. Oowada, H. Okumura, T. Kida, and A. Uchida, "Synchronization of bandwidth-enhanced chaos in semiconductor lasers with optical feedback and injection," Opt. Express **17**, 19536 (2009).
23. R. Takahashi, Y. Akizawa, A. Uchida, T. Harayama, K. Tsuzuki, S. Sunada, K. Arai, K. Yoshimura, and P. Davis, "Fast physical random bit generation

with photonic integrated circuits with different external cavity lengths for chaos generation," Opt. Express **22**, 11727 (2014).
24. B. Tromborg, H. Olesen, X. Pan, and S. Saito, "Transmission line description of optical feedback and injection locking for Fabry–Perot and DFB lasers," IEEE J. Sel. Top. Quantum Electron. **23**, 1875 (1987).
25. F.-Y. Lin, Y.-K. Chao, and T.-C. Wu, "Effective bandwidths of broadband chaotic signals," IEEE. J. Quantum Electron. **48**, 1010 (2012).
26. P. Li, Q. Cai, J. Zhang, B. Xu, Y. Liu, A. Bogris, K. A. Shore, and Y. Wang, "Observation of flat chaos generation using an optical feedback multi-mode laser with a band-pass filter," Opt. Express **27**, 17859 (2019).